International Journal of Pharmaceutics: X 7 (2024) 100252

Contents lists available at ScienceDirect

International Journal of Pharmaceutics: X

journal homepage: www.sciencedirect.com/journal/international-journal-of-pharmaceutics-x

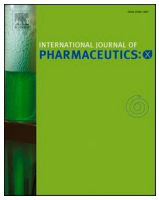

Stimuli-sensitive biomimetic nanoparticles for the inhibition of breast cancer recurrence and pulmonary metastasis

Dongjie Yang [a,1], Lan Zhang [b,1], Jiang Ni [a], Yang Ding [c], Anam Razzaq [d], Zaheer Ullah Khan [e], Haroon Iqbal [f], Yasmene Falah Alanazi [g], Naveed Ullah Khan [h,*], Rong Wang [b,*]

[a] Pathology Department& Department of Pharmacy, Affiliated Hospital of Jiangnan University, Wuxi 214000, P.R. China
[b] Wuxi School of Medicine, Jiangnan University, Wuxi 214000, P.R. China
[c] College of Pharmacy, Pharmaceutical Series, China Pharmaceutical University, Nanjing 210000, P.R. China
[d] College of Pharmaceutical Sciences, Soochow University, Suzhou, P.R. China
[e] Department of Pharmacy, COMSATS University Islamabad, Abbottabad Campus, Abbottabad, Pakistan
[f] The Eye Hospital, School of Ophthalmology and Optometry, Wenzhou Medical University, Wenzhou 325027, Zhejiang, P.R. China
[g] Department of Biochemistry, Faculty of Science, University of Tabuk, Tabuk 71491, Saudi Arabia
[h] College of Pharmaceutical Sciences, Zhejiang University of Technology, Hangzhou 310012, P.R. China

ARTICLE INFO

Keywords:
Biomimetic nanoparticles
Breast cancer recurrence
Pulmonary metastasis
Perfluorohexane
Doxorubicin

ABSTRACT

Biomimetic nanoparticles represent a promising avenue for mitigating rapid clearance by the reticuloendothelial system (RES); however, current challenges include insufficient tumour targeting, suboptimal adhesion, and inadequate localized drug release within tumour regions. These shortcomings contribute to persistent contests, such as recurrence and pulmonary metastasis, even with advanced breast cancer therapies. Stimuli-sensitive drug release can furbish the membrane coated nanoparticles for their efficiency against the stated problems. To enhance the efficacy of biomimetic nanoparticles in addressing these issues, we proposed a versatile, stimuli-responsive drug delivery system by encapsulating doxorubicin (Dox) and perfluorohexane (PFH) within poly (lactic-*co*-glycolic acid) (PLGA) nanoparticles, subsequently coated with macrophage-derived cell membranes. Within this framework, PFH serves as the mediator for ultrasonic (US)-irradiation-triggered drug release specifically within tumour microenvironment, while the macrophage-derived cell membrane coating enhances cell adhesion, enables immune evasion, and natural tumour-homing ability. The characterization assays and *in vitro* evaluations yielded encouraging results, indicating enhanced targeting and release efficiencies. *In vivo* studies demonstrated marked inhibitory effects on both breast cancer recurrence and pulmonary metastasis. The resulting data indicate that these engineered nanoparticles have notable potential for targeted delivery and controlled release upon US irradiation, thereby offering significant therapeutic efficacy against primary breast cancer, pulmonary metastasis, and recurrent malignancies. Our findings lay the groundwork for a novel clinical approach, representing an intriguing direction for ongoing investigation by oncologists.

1. Introduction

Breast cancer (BC) poses a significant challenge in contemporary healthcare, affecting populations in both developing and developed nations globally. Despite advancements in diagnostic methods and treatment modalities, breast cancer continues to be a leading cause of mortality (Wang et al., 2014), (Iqbal et al., 2021). While multiple treatment options exist such as surgical resection, chemotherapy, and radiotherapy, as well as emerging modalities like targeted therapy, immunotherapy, CAR-T cell therapy, and personalized medicine based on tumour genomics. The efficacy of these approaches is often compromised by recurrent malignancies and pulmonary metastases. Hence, there is an urgent need for sustained medical and clinical research to eradicate the recurrence and pulmonary metastasis of breast cancer, thereby offering a complete cure (Fang et al., 2014; Lopes et al., 2017; Wang et al., 2014).

Nanotechnology has emerged as a promising carrier for anticancer drug delivery, offering nanoparticles capable of traversing multiple

* Corresponding authors.
E-mail addresses: naveedkhan1676@hotmail.com (N.U. Khan), W0826R@outlook.com (R. Wang).
[1] These authors contributed equally to the work

https://doi.org/10.1016/j.ijpx.2024.100252
Received 12 February 2024; Received in revised form 26 April 2024; Accepted 1 May 2024
Available online 3 May 2024

biological barriers to facilitate enhanced tumour uptake and controlled drug release for maximal apoptosis. Nevertheless, an ideal nanocarrier should demonstrate extended residence time in circulation while evading clearance by the reticuloendothelial system (RES) (Gu and Hu, 2022; Oroojalian et al., 2021). Consequently, the meticulous design of nano-drug delivery systems should incorporate stabilizing strategies and optimal drug release mechanisms. Parameters such as particle size, surface charge, morphology, and surface modifications have been extensively investigated to prolong plasma residence time and augment drug accumulation in tumour-specific locales (Lv et al., 2021; Mu et al., 2017). Despite the advantages of PEGylated nanocarriers in extending plasma residence time, improving drug solubility, and reducing toxicity, their delivery efficacy remains suboptimal. Recent advancements have focused on cell membrane-coated nanoparticles, which inherently circumvent RES clearance, prolong plasma residence time, and elude immune surveillance (Khan et al., 2021; Yang et al., 2021). PEGylation, though widely accepted as a means to mitigate RES clearance, has been shown to induce 'accelerated blood clearance' phenomena in animal models (He et al., 2021). In contrast, membrane-coated nanoparticles show promise in enhancing both half-life and tumour adhesion. Innovative cell membrane coating technologies provide a straightforward top-down design approach, replicating the complex functionalities needed for effective biological interfacing (Chen et al., 2021). Notably, macrophage membranes offer several advantages, including prolonged blood circulation, enhanced antigen recognition for targeted delivery, improved cellular interactions, delayed drug release, and reduced *in vivo* toxicity (Zhang et al., 2018). Macrophages, a subset of lymphocytes, can recognize and engulf foreign particles and tumour cells, despite the absence of specific biomarkers that distinguish healthy cells (Kumari and Choi, 2022; Zhang et al., 2018). Utilizing macrophage membranes for nanoparticle surface modification represents a top-down approach, facilitated by rapid advancements in nanoscience and nanotechnology, that precisely mimics surface antigens from natural cells (Fang et al., 2018; Kumari and Choi, 2022; Zhang et al., 2018).

The primary objective of stimuli-responsive nanoparticles is to facilitate the targeted delivery, controlled release, and activation of therapeutic cargos in specific regions, such as tumour sites or intracellular compartments within tumour cells, in response to various triggers like enzymes, temperature changes, and ultrasonic (US) irradiation (Xu et al., 2017; Zhong et al., 2019). These stimulus-responsive functionalities enable temporally regulated or programmed drug release, enhanced tumour accumulation, ligand interactions, structural modifications of the nanoparticles, charge alterations, site-specific signalling, recognition of unique pathological markers, and tumour-oriented diagnostics (Mi, 2020; Ni et al., 2020).

PLGA, a biodegradable synthetic copolymer, is officially listed as a medical excipient in the United States Pharmacopoeia and has received FDA certification in the United States. Its superior entrapment efficiency and excellent physiological compatibility make it a prime choice over many other polymers (Khan et al., 2021). PLGA-based nanocarriers have the potential to prolong the half-life of bioactive medications in the circulatory system, preserve the biological functions of these medications, and enhance their stability against environmental factors, offering significant therapeutic benefits for patients on long-term medication regimens (Luo et al., 2019; Qin and Liu, 2022; Zhao et al., 2015). Meanwhile, perfluorohexane (PFH) has garnered attention in clinical trials due to its excellent biocompatibility and optimal phase-transition temperature of 56 °C, the most suitable among all known liquid Perfluorocarbons (PFCs). Stable at room temperature, PFH can be converted to a gas form through ultrasonic irradiation or localized temperature increases. It has been previously incorporated with PLGA to facilitate stimuli-sensitive (specifically, US-irradiation-based) release of encapsulated drugs (Mi, 2020; Xu et al., 2017; Zhong et al., 2019).

There is an urgent need for sustained medical and clinical research to eradicate the recurrence and pulmonary metastasis of breast cancer, thereby offering a complete cure. Here, we proposed an innovative approach by constructing nanosystem with PLGA and PFH, for stimuli-sensitive release of cytotoxic agent doxorubicin upon exposure to US irradiation in the tumour microenvironment. The nanoparticles were then coated with macrophage membrane, where adhesion increases the accumulation of nanoparticles in tumour regions. The designed nanocarrier system was aimed for improved drug targeting to breast cancer cells due membrane adhesion, increase accumulation of nanoparticles in tumour microenvironment to avoid the RES-clearance, to release the drug in tumour regions when exposed to US irradiations, to inhibit the breast cancer recurrence after surgical removal, and lungs metastases. This delivery tool may be helpful in the radical therapy of breast malignancies, and prevention of post-surgery breast tumour recurrence and lung metastases.

2. Materials and methods

2.1. Materials

PLGA (Poly (lactic-*co*-glycolic acid), Cat. 719,900) was acquired from Sigma-Aldrich (Shanghai, China). Polyvinyl alcohol (PVA) was acquired from Kuraray (Japan). MES buffer and PFH were procured from Aladdin Co., Ltd. (Shanghai, China). Doxorubicin was purchase from Beijing Yihe Biological Co. Ltd. (Beijing, China). 4,6-diamino-2-phenylindole (DAPI) was acquired from Sigma–Aldrich (St. Louis, MO, USA). Dulbecco's modified Eagle's medium (DMEM) was bought from Gibco (Tulsa, OK, USA). Other chemicals were acquired from Sigma-Aldrich unless otherwise specified and were used as received.

2.2. Methods

2.2.1. Preparation of M-PLGA-P-NPs/D

M-PLGA-P-NPs/D were synthesized using double emulsification solvent-evaporation technique as previously described with minor amendments (Khan et al., 2021). A total of 100 mg of PLGA was uniformly dispersed in 4 mL of dichloromethane (DCM) to prepare the organic (oily) phase. To this phase, 400 μL of PFH and 10 mg of Dox dissolved in 100 μL of DMSO were added under vortex. The mixture was then ultrasonicated for 1 min at 300 W (Sonics & Materials Inc., Newtown, Connecticut, USA). This prepared mixture was subsequently added to a PVA solution and ultrasonicated for another minute. Finally, 20 mL of 2% isopropyl alcohol was added to the solution, which was then stirred continuously for 2 to 4 h in an ice bath to complete the evaporation of the organic solvents. The NPs solution was centrifuged at 20,000 rpm (OPTIMAL-90 K, BECKMAN, USA) for 20 min at 4 °C to collect the solidified PLGA-P-NPs/D. These NPs were then washed three times with double-distilled water and freeze-dried. The freeze-dried NPs were stored at −20 °C for further use.

In our endeavour to fabricate M-PLGA-P-NPs/D using the extrusion technique, cultivated peritoneal macrophages derived from mice served as the foundation. Specifically, 1 mL of 4% thioglycolate broth media was administered intraperitoneally to a mouse 72 h prior to euthanasia. Following a thorough massage, 2 mL of DMEM medium in enterocoele was administered into the body. The DMEM containing macrophages was withdrawn and maintained in CO_2 humidified incubator. The collected macrophage ghost was produced by freezing and thawing a suspension of macrophages three times in liquid nitrogen. To harvest macrophage ghost, the lysate was centrifuged at 5000 rpm after being rinsed with buffer. After being sonicated for five minutes with a freshly manufactured nanoparticle solution the freshly created macrophage ghost was then extruded (Avanti mini extruder) through 400 nm and 100 nm polycarbonate porous membranes (Fang et al., 2014). The concentration of macrophage ghosts was quantified using protein quantification BCA kit assay, where the ratio of nanoparticles to macrophage ghosts was 1:10 (*w*/w).

2.2.2. Drug loading and entrapment efficiencies

The percent loading and entrapment efficiencies were measured by measuring amount of Dox in the given weight of NPs relative to the total amount of Dox added to the PLGA polymer. Particularly, 2 mg of the NPs were dissolved in DMSO and Dox was extracted. The amount of Dox was quantified *via* fluorescence microplate reader (Bioteck, USA). The percent entrapment efficiency and percent Dox loading were determined by means of the following formulas (Guo et al., 2018).

$$Drug\ loading\ (\%) = \frac{Dox\ in\ NPs}{Weight\ of\ NPs} x\ 100$$

$$Entrapment\ Efficiency\ (\%) = \frac{(Dox\ added - unencapsulated\ free\ Dox)}{Dox\ added} \times 100$$

2.2.3. Characterization of NPs

The coated and un-coated NPs were characterized for average size, zeta-potential, and poly- polydispersity index (PDI) through light dynamic scattering (DLS) technique *via* zeta-sizer (Malvern Instruments, Co., Ltd.). The surface morphology of the coated and un-coated NPs was evaluated *via* transmission electron microscope (JEM-2010, JEOL, Japan). Freshly developed samples were dissolved in filtered deionized water (1:10), then sonicated for one minute. A drop of the dispersion was applied to a copper grid and imaged (Iqbal et al., 2021). The *in vitro* drug release patterns were studied in phosphate buffer saline (PBS) at pH 5.0 containing 0.5% sodium dodecyl sulphate (SDS) with or without US-irradiations at specified time intervals. The specific amount of the NPs was resuspended in 1 mL PBS and enclosed firmly in dialysis bag (3500 MW) and dipped in 100 mL PBS in a conical flask, constantly oscillating at speed of 150 rpm. 1 mL of PBS was collected at particular time intervals and the medium was replaced with fresh PBS at the same amount (Khan et al., 2021). The Dox concentration was determined *via* fluorescence microplate reader (Bioteck, USA). Furthermore, to confirm the successful wrapping of macrophage membrane over M-PLGA-P-NPs/D, M-PLGA-P-NPs/D was denatured and resolved *via* 12% SDS-PAGE. The gel was disassembled and proteins in the gel were stained for 1 to 2 h in Coomassie blue staining solution. Then the gel was distained with 10% acetic acid, which was changed every 30 min until the background is clear (Gao et al., 2022).

2.2.4. Cell cultures and animals

Mouse-derived breast cancer cell lines (4 T1-luc) were procured from the Cell Bank of the Chinese Academy of Sciences (Shanghai, China). These cells were cultured in Dulbecco's modified Eagle's medium (DMEM) supplemented with 10% fetal bovine serum, 0.5% penicillin, and streptomycin, and maintained at 37 °C in a humidified atmosphere with 5% CO_2.

Female ICR and balb/c mice, weighing 20-25 g and 18-22 g respectively, were sourced from the Animal House of Jiangnan University, Wuxi, China and kept under standard conditions. For the subcutaneous xenograft breast cancer model, 2.5×10^6 4 T1-luc cells were injected subcutaneously in the proximal femur region of the mouse. All animals used in the experiments were taken care of in compliance with the Principles of Laboratory Animal Care and Guidance for the Care and Use of Laboratory Animals and kept under standard housing conditions. All the experiments were conducted after approval from the Institutional Animal Care and Use Committee (IACUC) of Jiangnan University (JN. No20211215b0480316[571]). All animal experiments were performed following the ARRIVE guidelines. The animals were anesthetized with intraperitoneal injection of (Ketamine/Xylazine mix 0.1 ml/10g mice body weight). Animals were euthanatized (cervical dislocation) as non-survival surgery & approved by Animal Institute Committee.

2.2.5. In vitro cell uptake studies

The *in vitro* targeting efficiency of the synthesized nanoparticles was assessed in 4 T1 cell lines. In a typical procedure, 4 T1 cells ($1x10^5$/well) were seeded in 6-well plates using DMEM supplemented with 10% FBS. Once the cells achieved normal morphology and confluency, they were treated with Dox-loaded nanoparticles at a concentration equivalent to 3 μg/mL Dox in DMEM. The cells were incubated for 2 h, either with or without subsequent US-irradiation (8 W, 3 min). Following incubation, cells were lysed using probe sonication, and Dox was extracted with DMSO. Dox quantities were then determined *via* fluorescence microplate reader (Bioteck, USA) at wavelengths of 470/560 nm. A blank sample was also included to account for and subtract background interference from the test samples. Subsequently, the uptake of the nanoparticles by 4 T1 cells was investigated. For this, 4 T1 cells were cultured in 6-well plates and exposed to Dox/NPs. Cellular uptake of Dox was then quantified using flow cytometry (Khan et al., 2021; Xu et al., 2017).

2.2.6. In vitro cytotoxicity

The 4 T1 cells were harvested in 96-well culture plates at a confluence of 5000 cells/well, after 24 h, they were exposed to blank NPs over a 48-h period to evaluate the cytotoxicity. Afterward, cell growth was computed through the standard MTT assay. The same MTT assay was performed for free Dox and various groups of NPs with/ without US-irradiation (8 W, 3 min) after 2 h incubation to evaluate the *in vitro* antitumour effects cell growth and IC_{50} value were reported using the standard MTT assay (Wang et al., 2014).

2.2.7. In vivo imaging and %injected dose of NPs in subcutaneous tumour bearing mice

Tumour bearing mice were arbitrarily alienated into four groups ($n = 4$) and IV administered with free IR780, and IR780 loaded NPs at the dosing 0.75 mg/kg IR780. After 24 h of injection, the animals were given anaesthesia and envisaged *via* IVIS imaging system (Caliper, CA, USA). Where the fluorescence intensity of the NPs localized in tumour regions was counted using Living Image 3.0 (Caliper, CA) (Ni et al., 2020).

To conclude the percent injected dose (%ID), Free IR780, PLGA-P-NPs/IR780, and M-PLGA-P-NPs/IR780 were intravenously administered into the tumour bearing mice at the dose of 0.75 mg/kg IR780. The 24 h post-injection, the mice were sacrificed, the major organs and tumours were excised, and homogenized. Then the minced tissues (20 mg) were intruded in 180 μL DMSO to extract IR780. IR780 was quantified using the fluorescence intensity of the IR780 was counted and compared with standard curve using Living Image 3.0 (Caliper, CA) (Tecan) (Ni et al., 2020).

2.2.8. Pharmacokinetics and distribution of NPs in normal mice

Sixteen ICR mice were at random divided into four groups. Group 1 was IV administered with free IR780, and second group was administered with PLGA-NPs/IR780, group 3 received PLGA-P-NPs/IR780, and group 4 received M-PLGA-P-NPs/IR780 at 0.75 mg/kg IR780 intravenous dose. The 20 μL of blood samples were taken at 1 min, 2 h, 4 h, 8 h, 12 h, 24 h, 48 h, and 72 h from the vein of the mouse tail, and mixed with 180 μL DMSO to extract IR780. All the blood samples were immediately transferred into the 96 well plates for NIR fluorescence images through IVIS system (Caliper, CA, USA), and the intensity was counted using Living Image 3.0 (Caliper, CA, USA) (Ni et al., 2020).

2.2.9. In vivo treatments of the tumour bearing mice

To study the *in vivo* therapeutic efficiency of the designed US-irradiation sensitive NPs, tumour carrying mice were distributed at random in various groups (PBS, free Dox, PLGA-NPs/D, PLGA-P-NPs/D, and M-PLGA-P-NPs/D, $n = 8$). The PBS, free drug, and NPs were intravenously injected twice/week at the dose of 3 mg/kg Dox with US-irradiation. On alternate every 3rd day, the volume of the tumours in every group were measured according to the equation given below. In the same way, the mice body weights were calculated for 21-days. The percent survival was calculated for all the groups and statistical significance was calculated (Qian et al., 2018).

$V = A\ x\ B^2/2.$

Where, A: maximum diameter of the tumour; B: minimum diameter of the tumour.

To evident the tumour recurrence reticence and lungs metastases, another series of tumour bearing mice were at random divided for treatments after the surgical removal of tumours. The percent survival was calculated for all the groups and statistical significance was calculated. At random, mice were intraperitoneally injected with luciferase 100 μL (10 mg/mL) and sacrificed, subsequently their lungs were visualized under IVIS system for evidencing the Lung metastasis.

2.2.10. Systemic toxicities evaluations

To study the systemic toxicity of the NPs in physiological system, female ICR mice were at random divided into two groups ($n = 4$). One group was IV administered with PBS and another group with M-PLGA-P-NPs/D (3 mg Dox/kg). After 24 h post injection, blood was collected through submandibular vein. Serum was separated from the blood sample by means of centrifugation. To evaluate liver and kidney safety, the serum was imperilled to alanine-amino-transferase (ALT), and aspartate-amino-transferase (AST) testing using commercial kits (Sigma MAK055 and MAK052), creatinine (Cre), and blood-urea-nitrogen (BUN) as biomarkers of kidney and liver function (MultiSciences, Hangzhou, China). PBS-treated mice were used as controls (Qian et al., 2018).

2.2.11. Hematoxylin and Eosin (H&E) staining

Hematoxylin and eosin, two histological stains, where the extracellular-matrix and cytoplasm are stained pink by eosin and nucleus-stained purple by hematoxylin. It gives microscopic visual to study any difference with the control group. The major organs were excised and fixed with PFA for 24 h to create H&*E*-stained slices. Then images were taken, analysed, and reported (Zhong et al., 2019).

2.2.12. Statistical analysis

All the experimentations were done with least of three replications and data were reported as mean ± SD. Unpaired student *t*-test was applied for the comparison of any two results. For treatment related survival significance, One-way ANOVA analysis was done using GraphPad prism. $^*P < 0.05$, $^{**}P < 0.01$, $^{***}P < 0.001$ were considered statistically significant.

3. Results and discussion

3.1. Nanoparticle's synthesis and characterizations

The synthesis of the nanoparticles is elucidated in the Scheme 1, where the Dox encapsulated PLGA and PFH NPs were synthesized. To ensure accumulation in the tumour cells and escape from RES, the PLGA-P-NPs/D were coated with macrophage cell-membrane. The hydrodynamic diameter, PDI, and zeta-potential of the PLGA-P-NPs/D and M-PLGA-P-NPs/D were measured through Zetasizer. The mean diameter was found to be approximately ≈134 nm and ≈140 nm for PLGA-P-NPs/D and M-PLGA-P-NPs/D (Fig. 1A), respectively. The analysis showed that macrophage cell-membrane coating didn't affects the particles size distribution significantly. The PDI of both the NPs were <0.2 (Fig. 1B), showing excellent uniformity while the zeta-potential of the M-PLGA-NPs-P/D was slightly more negative (Fig. 1B) that might be due to the negatively charged macrophage cell-membrane coating (Fang et al., 2018; Shi and Tabas, 2022). The nanoparticles were incubated in 10% serum albumin up to 12 days and were analysed for PDI and particle size diameter to study the particulate stability of the nanoparticles in the physiological circulation. The supporting **Fig. S1** shows that there was no significant increase in the particle size (**Fig. S1A**) and PDI (**Fig. S1B**) of the NPs, that declares the Dox loaded M-PLGA-P/D NPs as stable formulation physically, which can be administered for prolonged circulation in the physiological fluids (Fang et al., 2014). The TEM images in Fig. 1C and D showed spherical surface morphology, where the

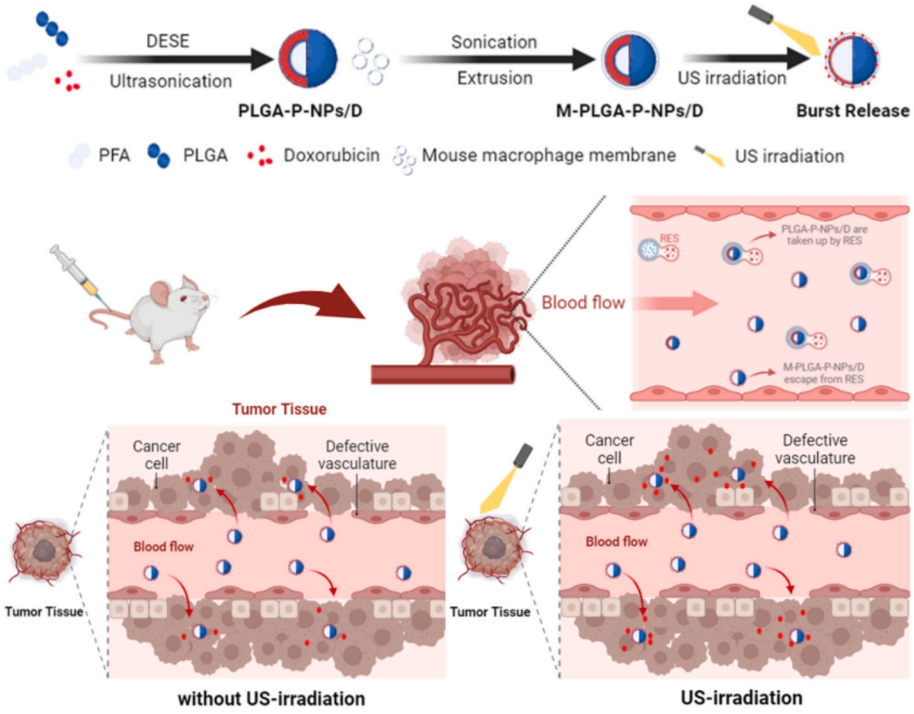

Scheme 1. M-PLGA-P-NPs/D are prepared by double emulsion solvent evaporation technique and coated with macrophage membrane though extrusion. Once in the bloodstream, M-PLGA-P-NPs/D evade the reticuloendothelial system (RES) and accumulate in the tumour microenvironment *via* cell membrane adhesion. US-irradiation triggers the tumour-specific release of Dox, serving to eliminate tumour cells and inhibit both lung metastasis and breast cancer recurrence. The scheme was created using BioRender web https://app.biorender.com/.

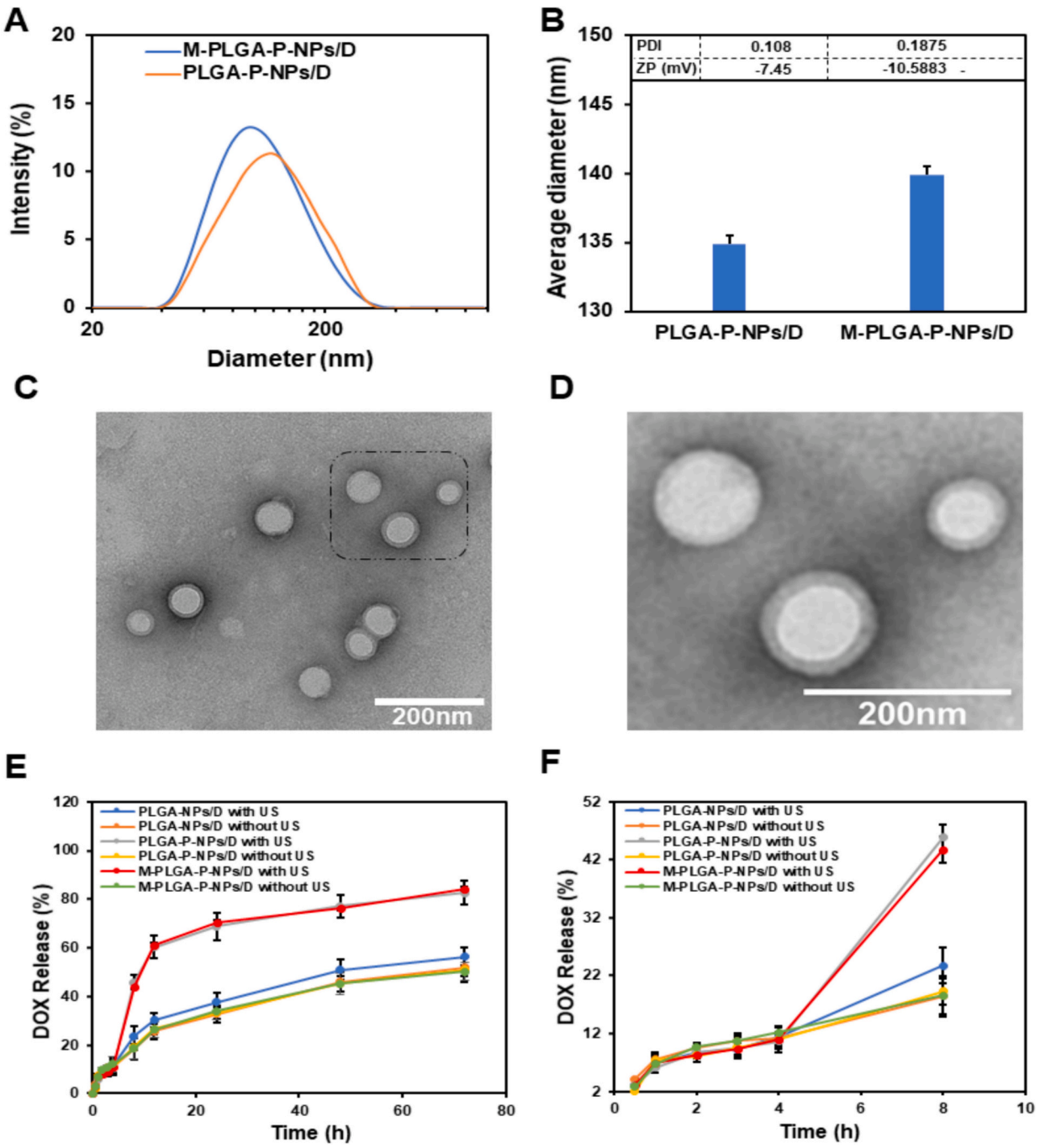

Fig. 1. Physicochemical characterization. Particle size distribution of PLGA-P/D and M-PLGA-P-NPs/D (A). Hydrodynamic particle sizes, zeta-potential, and PDI of PLGA-P-NPs/D and M-PLGA-P-NPs/D (B). TEM images M-PLGA-P/D NPs (C). Zoomed dotted section of TEM image in (C) (D). Release profile with or without US irradiations at pH 5.0. The sample irradiations were started after 4 h (E, F). Data are presented as mean ± SD, $n = 3$.

presence of the membrane coating being evident from the heightened contrast. The TEM analysis reflected the mean particle size of approximately 95 nm for M-PLGA-P-NPs/D. Macrophage membranes and PLGA-P-NPs/D were applied at optimum ratio to construct PLGA-P-NPs/D, the SDS–PAGE confirmed the successful coating of the macrophage membranes (**Fig. S2**). The release pattern of Dox was studied in PLGA -NPs/D, PLGA-P-NPs/D, and M-PLGA-P-NPs/D at acidic environment. The release patterns were same for all the NPs without US-irradiations at pH 5.0. The sample was focused with US-irradiations after 4 h, where the release of Dox from PLGA-P-NPs/D and M-PLGA-P-NPs/D with US-irradiations were recorded almost 2.2 to 2.4 fold higher than PLGA-NPs/D with US, PLGA-NPs/D without US, PLGA-P-NPs/D without US, M-PLGA-P-NPs/D without US, after 8 h, while it was recorded 2 fold higher at 24 h at pH 5.0 (Fig. 1E, F). The release studies showed that PLGA-P-NPs/D with US irradiation cause burst release. The data confirm the further testing of the NPs for *in vitro* and *in vivo* studies.

3.2. *In vitro cellular uptake and anti-tumour efficiency*

The nanoparticles were next evaluated for *in vitro* cellular uptake studies. The PLGA-NPs/D, PLGA-P-NPs/D, and M-PLGA-P-NPs/D with or without US irradiations were studied for Dox uptake in the 4 T1 cell lines. The PLGA-NPs/D and PLGA-P-NPs/D showed comparable cell uptake while M-PLGA-P-NPs/D showed significantly higher cell uptake

in flow cytometry results (Fig. 2A, B). The same results were obtained in Fig. 2C, when analysed with or without US-irradiations (Zhong et al., 2019). These results prove that US irradiation can cause burst drug release in thermo sensitive NPs (from Fig. 1E) but not affect the cell uptake. So, the enhanced cell uptake might be due to macrophage cell membrane coating (Kumari and Choi, 2022). These results proved the potential benefits of macrophage membrane coating for drug targeting.

Furthermore, the cells viability was evaluated to confirm the safety of the nanocarrier, and antitumour efficacy of drug loaded nanoparticles through standard MTT assay. The supporting **Fig. S3** showed negligible cytotoxicity towards 4 T1 cells that confirm the physiological safety of the nanocarriers. On other hand the results from MTT assay (Fig. 2D-F) shows promising cytotoxic effects for free Dox and M-PLGA-P-NPs/D. The IC_{50} calculated for free Dox was approximately 0.23 μg/mL, and ~ 0.1995 μg/mL for M-PLGA-P-NPs/D. The significantly lower IC_{50} for M-PLGA-P-NPs/D as compared to free Dox is due to burst release of the Dox from nanoparticle's core upon US irradiations (Xu et al., 2017; Zhong et al., 2019). The antitumour studies confirm cytotoxicity for cancer cells and declared that nanoparticles can be used for *in vivo* evaluations.

3.3. Biodistribution and Pharmacokinetics

To check the *in vivo* localization of the nanoparticles in tumour regions, IR780 loaded nanoparticles were administered intravenously and images were taken through IVIS system. The fluorescence intensity was counted using Living Image 3.0 (Caliper). The images and fluorescence intensity (Fig. 3A, B) showed that there was an obvious localization of the of M-PLGA-P-NPs/IR780 in tumour regions as compared to the PLGA-NPs/ IR780 and free IR780. The study revealed that membrane coating can promisingly prolong the nanoparticle's circulation as well as promote drug targeting to tumour regions.

The IR780 loaded nanoparticles were administered intravenously to normal ICR mice to check distribution in normal mice, the major organs (heart, liver, spleen, kidneys, and lungs) were excised, and the images were taken through IVIS system, and the fluorescence was quantified through Living Image 3.0 (Caliper). The **Fig. S6**, shows the distribution pattern in order of liver, spleen, kidneys, lungs, and heart. The distribution pattern was almost similar for all the nanoparticles. The plasma curve shows comparatively prolonged circulation time (Fig. 3C). Furthermore, percent injected dose was calculated for all the nanoparticles (Fig. 3D), where all the major organs showed same distribution order. There was approximately same liver distribution for all the nanoparticles, confirming the same dose administration. While there was significantly higher percent ID for M-PLGA-P-NPs/IR780 US-irradiated NPs (~4%) compared with PLGA-NPs/ IR780 and PLGA-P-NPs/IR780 US-irradiated NPs (~2.2%). These studies again proved the promising tumour targeting and prolonged circulation. Therefore, the designed US responsive nanoparticles can be unique approach for radical elimination of breast cancer and prevent lungs metastasis after the surgical removal of breast tumour.

The goal of the pharmacokinetics investigations was to determine the distribution patterns of M-PLGA-P-NPs/ IR780 throughout the blood (Qian et al., 2018). Where a different distribution pattern was found for M-PLGA-P-NPs/IR780 as compared to the free IR780 (Fig. 3C), that cleared quickly. The pharmacokinetic data in Table 1 showed that, M-PLGA-P-NPs/IR780 were cleared in a sustained manner and exhibited large area under the curve from time 0 to time t (AUC_{0-t}), lengthier mean residence time (MRT_{0-t}) and improved half-life time ($t_{1/2}$), with lower clearance (CL). The data declared M-PLGA-P/IR780-NP's sustained circulation behaviour, that is valuable for drug localization in tumour regions. In addition, all other NPs showed comparable blood distribution profiles with statistically insignificant difference in pharmacokinetic data.

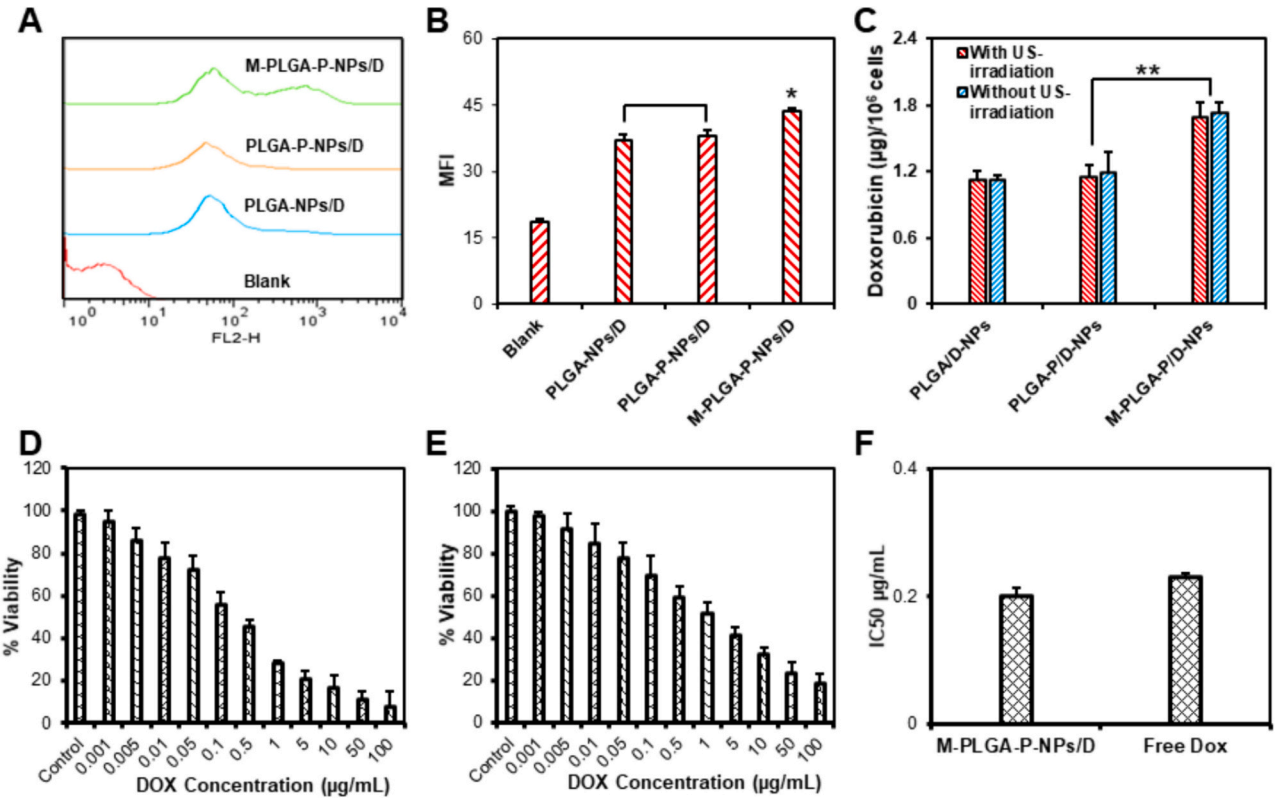

Fig. 2. *In vitro* evaluations. Cellular uptake in 4 T1 cells analysed by flow cytometry without US-irradiations (A, B). Cellular uptake in 4 T1 cells with or without US-irradiations (C). Cell viability of free M-PLGA-P-NPs/D with US-irradiations (D), DOX with US-irradiations (E), and their IC50 value (F) determined by standard MTT assay. Data are presented as mean ± SD. Where, P* < 0.05, P** < 0.01, P*** < 0.001.

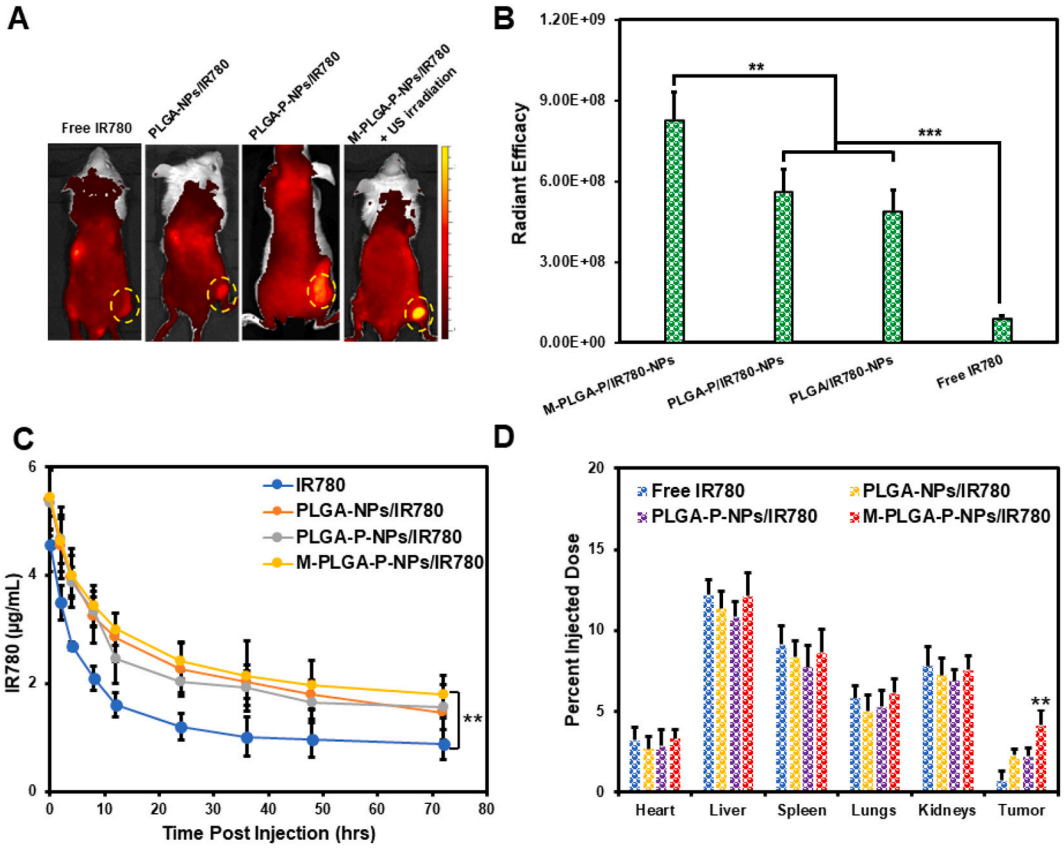

Fig. 3. Biodistribution of the nanoparticles. The IVIS image of tumour bearing mice injected with various IR780 nanoparticles (A) and quantification of IVIS images (B). Plasma time curve of various NPs in normal mice (C). Percent injected dose of various nanoparticles in major organs and tumour in tumour bearing mice (D). Data are presented as mean ± SD, $n = 4$. Where, P* < 0.05, P** < 0.01, P*** < 0.001.

Table 1
Pharmacokinetic parameters of M-PLGA-P-NPs/IR780 in normal ICR mice.

Parameter	Unit	IR780	M-PLGA-P-NPs/IR780
$t_{1/2}$	h	13.37 ± 0.82	***34.189 ± 3.41
CL	(μg)/(μg/ml)/h	6.06 ± 0.97	1.995 ± 0.23
AUC_{0-t}	μg/ml*h	72.44 ± 1.31	173.138 ± 0.67
AUC_{0-inf}	μg/ml*h	74.22 ± 1.89	***225.529 ± 7.12
MRT	h	19.29 ± 1.62	***49.325 ± 1.92

3.4. *In vivo* therapeutic efficacy

After excellent physicochemical characterization and *in vitro* evaluations, the nanoparticles were checked for the *in vivo* therapeutic efficiency. The vehicle (PBS), free Dox, PLGA-NPs/D, PLGA-P-NPs/D, and M-PLGA-P-NPs/D were injected intravenously at the dose of 3 mg/kg Dox through tail vein of the Balb/c mice along with US irradiations after the inoculation of tumour cells. The tumour volume and weight of the mice were calculated on alternate days (Fig. 4A, B). The tumour volume was significantly inhibited by M-PLGA-P-NPs/D as compared to control and other nanoparticles (**Fig. S4**). The weight analysis showed no obvious decrease in average weight of the treated mice as compared to free Dox and other nanoparticles. The survival curve showed significant increase in the survival of treated mice when compared with other nanoparticles (Fig. 4C). The superb therapeutic efficiency was seen in treatments group for designed nanoparticles loaded with Dox. The median survival calculated was found to be 34.5 days, 54 days, 51 days, and 51 days for PBS, free Dox, PLGA-NPs/D, and PLGA-P-NPs/D while there was an undefined increase in the survival for M-PLGA-P-NPs/D. The efficiency might be attribute due to prolonged circulation and targeted delivery to tumour regions owing to macrophage membrane coating as well as US irradiation responsive release in tumour regions (He et al., 2021; Zhang et al., 2018).

Next tumour mice were at random divided in various groups and the tumours were surgically removed, and then intravenously treated with PBS, free Dox, PLGA-NPs/D, PLGA-P-NPs/D, and M-PLGA-P-NPs/D (with US irradiation). Then studied for median survival. The median survival calculated was found to be 36 days, 33 days, 45 days, 51 days, and 69 days for PBS, free Dox, PLGA-NPs/D, PLGA-P-NPs/D, and M-PLGA-P-NPs/D as shown in Fig. 4D. There was an obvious increase noted for Dox loaded M-PLGA-P-NPs/D after surgical removal of tumours (**Fig. S5**). The significance in treatment efficiency might be owing to macrophage membrane and US irradiation responsive release. The Lung metastasis was qualitatively and quantitatively analysed by IVIS system, the fluorescence intensity was also quantified using Living Image 3.0 (Caliper) in PBS treated mice and M-PLGA-P-NPs/D (US irradiated) mice of the same treatments groups as shown in Fig. 4E, F. Both qualitative images and quantitive calculations showed obvious metastasis in PBS treated group while there was no lungs metastasis in M-PLGA-P-NPs/D (US irradiated) treated group.

3.5. *Evaluation of systemic safety*

PLGA is generally considered safe for *in vivo* use and suitable for cytotoxic drug delivery. However, the safety evaluation is prior recommendation to check whether the nanocarriers is compatible with physiological system and organ system or not. The Dox loaded M-PLGA-P-NPs/D were injected into the ICR mice and evaluated for liver and kidney safety tests (ALT, AST, BUN, and CRE) against PBS group (Khan et al., 2021; Qian et al., 2018). H&E staining's were endorsed to detect the microscopic differences in the morphology of major organs. The

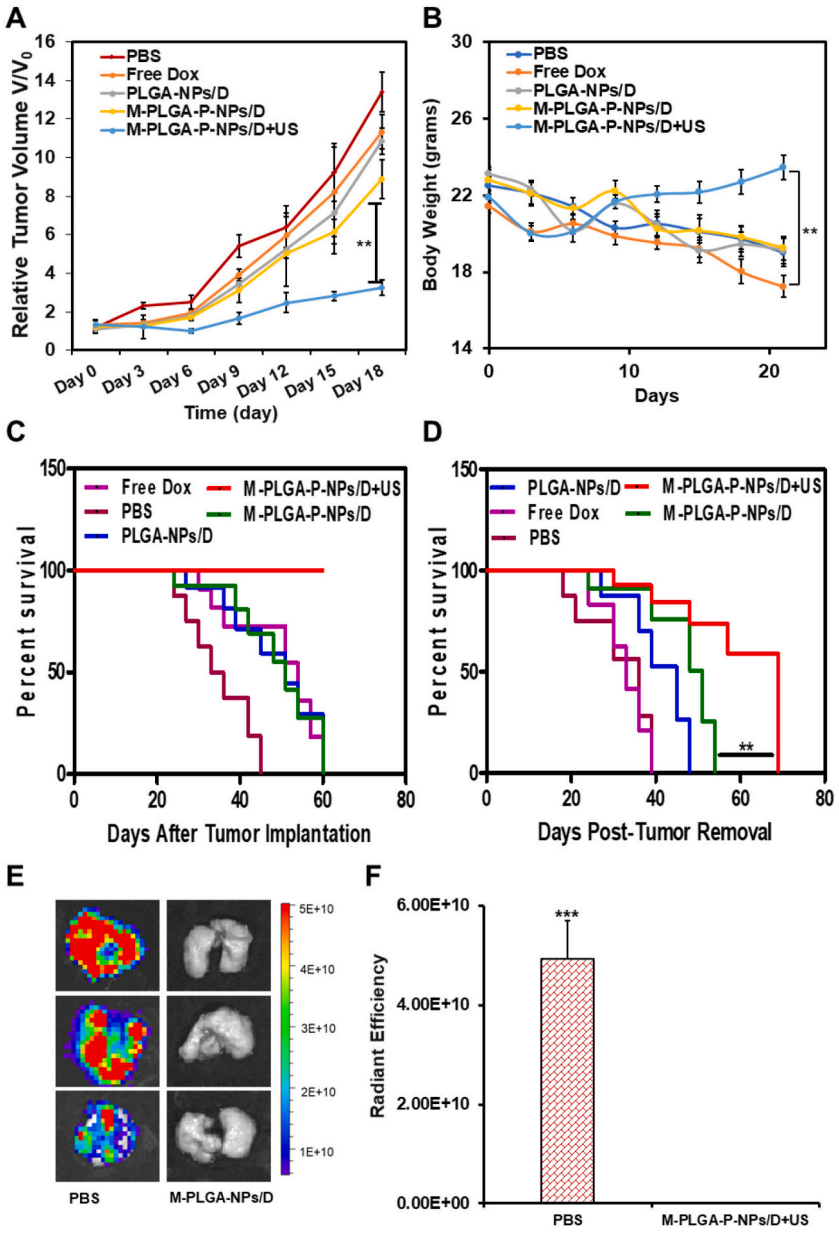

Fig. 4. *In vivo* therapeutic efficacy. The relative tumour volume measured for various groups (A). The average weight measured for the various groups (B). The median survival was calculated before surgery for the various nanoparticles groups (C). The median survival was calculated after surgery for the various nanoparticles groups (D). The Lung metastasis was qualitatively and quantitatively analysed by IVIVS system linked with software IVIVS lumina 3.0 in PBS treated mice and M-PLGA-P-NPs/D (US irradiated) mice of the same treatments groups (E, F). Data are presented as mean ± SD, $n = 8$. Where, P* < 0.05, P** < 0.01, P*** < 0.001.

ALT, AST, BUN, and CRE tests were comparable for PBS group and Dox loaded M-PLGA-P-NPs/D that proved promising safety for liver and kidney (Fig. 5A-D). The H&E staining images showed no obvious changes for PBS group and Dox loaded M-PLGA-P-NPs/D (Fig. 5E). Biosafety studies confirmed that Dox loaded M-PLGA-P-NPs/D are safe for the systemic administration and exhibits no obvious toxicity for the major organs.

4. Conclusion

Here, we provided a novel approach to treat breast cancer and inhibition of lungs metastasis with the designed targeted nanoparticle's drug delivery system. The outcomes for potential localization in the tumour regions, and robust release with US irradiations were promising. The significant therapeutic efficacy of the designed nanoparticles was achieved against breast cancer, breast cancer lungs metastasis, and breast cancer recurrence. In future studies, the research study may be diversified towards multiple animal's models to verify the clinical efficacy. Finally, we have constructed an excellent clinical regimen for the radical treatment of breast cancer that can be an interesting effort for readers.

Ethical approval statement

All animals used in the experiments were taken care of in compliance with the Principles of Laboratory Animal Care and Guidance for the Care and Use of Laboratory Animals and kept under standard housing conditions. All the experiments were conducted after approval from the Institutional Animal Care and Use Committee (IACUC) of Jiangnan University (JN. No20211215b0480316[571]). All animal experiments

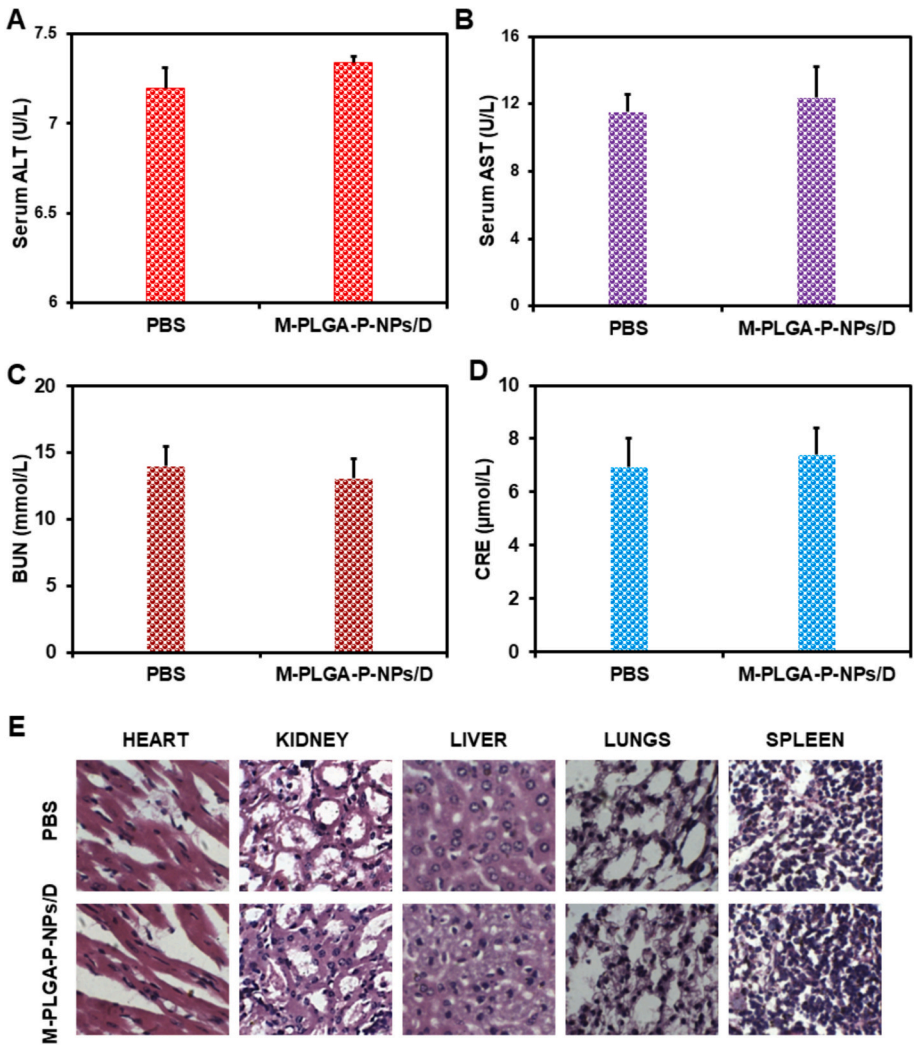

Fig. 5. Systemic safety. ALT, alanine transaminase (A). AST, aspartate aminotransferase (B). BUN, blood urea nitrogen (C). CRE, creatinine clearance (D). H&E Staining of the excised organs of normal mice treated with PBS and Dox loaded M-PLGA-P-NPs (Scale bar: 100μm). Data are presented as mean ± SD, $n = 4$.

were performed following the ARRIVE guidelines and authors were adhered to the ARRIVE guidelines. The animals were anesthetized with intraperitoneal injection of Ketamine/Xylazine mix (0.1 ml/10 g mice body weight). Animals were euthanatized (cervical dislocation) as non-survival surgery & approved by Animal Institute Committee. The ethical approval was obtained for animals' experiments.

Funding

The study was supported by Wuxi Municipal Health Commission Youth Research Project (No: Q202230) and Top Talent Support Program for young and middle-aged people of Wuxi Health Committee (BJ2023063).

CRediT authorship contribution statement

Lan Zhang: Formal analysis, Data curation, Conceptualization. **Jiang Ni:** Visualization, Validation, Software, Data curation. **Yang Ding:** Software, Methodology, Formal analysis, Data curation, Conceptualization. **Anam Razzaq:** Methodology, Investigation, Formal analysis, Data curation, Conceptualization. **Haroon Iqbal:** Methodology, Investigation, Formal analysis, Data curation. **Yasmene Falah Alanazi:** Funding acquisition, Formal analysis, Data curation, Conceptualization. **Naveed Ullah Khan:** Writing – review & editing, Writing – original draft, Supervision, Methodology, Investigation, Conceptualization. **Rong Wang:** Writing – review & editing, Writing – original draft, Funding acquisition, Formal analysis, Data curation, Conceptualization.

Declaration of competing interest

All the authors read the manuscript before submission and declared that they have no conflict of interest.

Data availability statement

The data that support the findings of this study are available from the corresponding author, [N.U.K], upon reasonable request.

Appendix A. Supplementary data

Supplementary data to this article can be found online at https://doi.org/10.1016/j.ijpx.2024.100252.

References

Chen, C., Song, M., Du, Y., Yu, Y., Li, C., Han, Y., Feng, S., 2021. Tumor-associated-macrophage-membrane-coated nanoparticles for improved photodynamic immunotherapy. Nano Lett. 21, 5522–5531. https://doi.org/10.1021/acs.nanolett.1c00818.

Fang, R.H., Hu, C.M.J., Luk, B.T., Gao, W., Copp, J.A., Tai, Y., Zhang, L., 2014. Cancer cell membrane-coated nanoparticles for anticancer vaccination and drug delivery. Nano Lett. 14 (4), 2181–2188. https://doi.org/10.1021/nl500618u.

Fang, R.H., Kroll, A.V., Gao, W., Zhang, L., 2018. Cell Membrane Coating Nanotechnology. Adv. Mater. 30 (23), e1706759 https://doi.org/10.1002/adma.201706759.Cell.

Gao, C., Chen, Y., Cheng, X., Zhang, Y., Zhang, Y., Wang, Y., Gu, J., 2022. A novel structurally identified epitope delivered by macrophage membrane-coated PLGA nanoparticles elicits protection against *Pseudomonas aeruginosa*. J. Nanobiotechnol. 20 (532), 1–14. https://doi.org/10.1186/s12951-022-01725-x.

Gu, F., Hu, C., 2022. Tumor microenvironment multiple responsive nanoparticles for targeted delivery of doxorubicin and CpG against triple-negative breast cancer. Int. J. Nanomedicine 17, 4401–4417.

Guo, Q., Chang, Z., Khan, N.U., Miao, T., Ju, X., Feng, H., Han, L., 2018. Nanosizing noncrystalline and porous silica material?Naturally occurring opal shale for systemic tumor targeting drug delivery. ACS Appl. Mater. Interfaces 10, 25994–26004.

He, Y., Fernandes, R., Ara, D., Cruz, L.J., Eich, C., 2021. Functionalized nanoparticles targeting tumor-associated macrophages as cancer therapy. Pharmaceutics 13, 1670.

Iqbal, H., Razzaq, A., Uzair, B., Ain, N.U., Sajjad, S., Khan, N.U., Menaa, F., 2021. Breast cancer inhibition by biosynthesized titanium dioxide nanoparticles is comparable to free doxorubicin but appeared safer in BALB / c mice. Materials 14, 3155.

Khan, N.U., Ni, J., Ju, X., Miao, T., 2021. Escape from abluminal LRP1-mediated clearance for boosted nanoparticle brain delivery and brain metastasis treatment. Acta Pharm. Sin. B 11 (5), 1341–1354. https://doi.org/10.1016/j.apsb.2020.10.015.

Kumari, N., Choi, S.H., 2022. Tumor-associated macrophages in cancer : recent advancements in cancer nanoimmunotherapies. J. Exp. Clin. Cancer Res. 41 (68), 1–39. https://doi.org/10.1186/s13046-022-02272-x.

Lopes, C.M., Dourado, A., Oliveira, R., 2017. Phytotherapy and nutritional supplements on breast cancer. Biomed. Res. Int. 2017, 42. https://doi.org/10.1155/2017/7207983.

Luo, Y., Xu, D., Gao, X., Xiong, J., Jiang, B., Zhang, Y., Wang, Y., 2019. Nanoparticles conjugated with bacteria targeting tumors for precision imaging and therapy. Biochem. Biophys. Res. Commun. https://doi.org/10.1016/j.bbrc.2019.05.074.

Lv, L., Shi, Y., Wu, J., Li, G., 2021. Nanosized drug delivery systems for breast cancer stem cell targeting. Int. J. Nanomedicine 16, 1487–1508.

Mi, P., 2020. Theranostics stimuli-responsive nanocarriers for drug delivery, tumor imaging, therapy and theranostics. Theranostics 10 (10), 4557–4588. https://doi.org/10.7150/thno.38069.

Mu, Q., Wang, H., Zhang, M., 2017. Nanoparticles for imaging and treatment of metastatic breast cancer. Expert Opin. Drug Deliv. 14 (1), 123–136. https://doi.org/10.1080/17425247.2016.1208650.Nanoparticles.

Ni, J., Miao, T., Su, M., Ullah, N., Ju, X., Chen, H., 2020. PSMA-targeted nanoparticles for specific penetration of blood-brain tumor barrier and combined therapy of brain metastases. J. Control. Release 10. https://doi.org/10.1016/j.jconrel.2020.10.023.

Oroojalian, F., Beygi, M., Baradaran, B., Mokhtarzadeh, A., Shahbazi, M., 2021. Immune cell membrane-coated biomimetic nanoparticles for targeted cancer therapy. Small 17, 2006484. https://doi.org/10.1002/smll.202006484.

Qin, H., Liu, Y., 2022. Drug release from gelsolin-targeted phase-transition nanoparticles triggered by low-intensity focused ultrasound. Int. J. Nanomedicine 17, 61–71.

Shi, J., Tabas, I., 2022. Macrophage-targeted nanomedicine for the diagnosis and treatment of atherosclerosis. Nat. Rev. Cardiol. 19, 228–249. https://doi.org/10.1038/s41569-021-00629-x.

Wang, D., Xu, Z., Yu, H., Chen, X., Feng, B., Cui, Z., Li, Y., 2014. Biomaterials treatment of metastatic breast cancer by combination of chemotherapy and photothermal ablation using doxorubicin-loaded DNA wrapped gold nanorods. Biomaterials 1–11. https://doi.org/10.1016/j.biomaterials.2014.05.094.

Xu, J., Zhou, J., Zhong, Y., Zhang, Y., Liu, J., Chen, Y., Guo, D., 2017. Phase transition nanoparticles as multimodality contrast agents for the detection of thrombi and for targeting thrombolysis: in vitro and in vivo experiments. ACS Appl. Mater. Interfaces 9 (49), 42525–42535. https://doi.org/10.1021/acsami.7b12689.

Yang, Z., Yao, J., Wang, J., Zhang, C., Cao, Y., Hao, L., Tian, Y., 2021. Ferrite-encapsulated nanoparticles with stable photothermal performance for multimodal imaging-guided atherosclerotic plaque neovascularization therapy. Biomater. Sci. 9, 5652–5664. https://doi.org/10.1039/d1bm00343g.

Zhang, Y., Cai, K., Li, C., Guo, Q., Chen, Q., He, X., Zhang, Y., 2018. Macrophage-membrane-coated nanoparticles for tumor-targeted chemotherapy. Nano Lett. https://doi.org/10.1021/acs.nanolett.7b05263.

Zhao, Y., Song, W., Wang, D., Ran, H., Yao, Y., Wang, Z., Li, P., 2015. Phase-shifted PFH@PLGA/Fe3O4 nanocapsules for MRI/US imaging and photothermal therapy with near-infrared irradiation. ACS Appl. Mater. Interfaces. https://doi.org/10.1021/acsami.5b01873.

Zhong, Y., Zhang, Y., Xu, J., Zhou, J., Liu, J., Ye, M., Guo, D., 2019. Low-intensity focused ultrasound-responsive phase-transitional nanoparticles for thrombolysis without vascular damage: a synergistic nonpharmaceutical strategy. ACS Nano 13 (3), 3387–3403. https://doi.org/10.1021/acsnano.8b09277.